

# Cutaneous $\alpha$ -Synuclein Signatures in Patients With Multiple System Atrophy and Parkinson Disease

Christopher Gibbons, MD, MMSc,\* Ningshan Wang, PhD,\* Sharika Rajan, MD, Drew Kern, MD, Jose-Alberto Palma, Horacio Kaufmann, MD, and Roy Freeman, MD

*Neurology*® 2023;100:e1529-e1539. doi:10.1212/WNL.0000000000206772

## Correspondence

Dr. Freeman  
rfreeman@  
bidmc.harvard.edu

## Abstract

### Background and Objectives

Multiple system atrophy (MSA) is a progressive neurodegenerative disorder caused by the abnormal accumulation of  $\alpha$ -synuclein in the nervous system. Clinical features include autonomic and motor dysfunction, which overlap with those of Parkinson disease (PD), particularly at early disease stages. There is an unmet need for accurate diagnostic and prognostic biomarkers for MSA and, specifically, a critical need to distinguish MSA from other synucleinopathies, particularly PD. The purpose of the study was to develop a unique cutaneous pathologic signature of phosphorylated  $\alpha$ -synuclein that could distinguish patients with MSA from patients with PD and healthy controls.

### Methods

We studied 31 patients with MSA and 54 patients with PD diagnosed according to current clinical consensus criteria. We also included 24 matched controls. All participants underwent neurologic examinations, autonomic testing, and skin biopsies at 3 locations. The density of intraepidermal, sudomotor, and pilomotor nerve fibers was measured. The deposition of phosphorylated  $\alpha$ -synuclein was quantified. Results were compared with clinical rating assessments and autonomic function test results.

### Results

Patients with PD had reduced nerve fiber densities compared with patients with MSA ( $p < 0.05$ , all fiber types). All patients with MSA and 51/54 with PD had evidence of phosphorylated  $\alpha$ -synuclein in at least one skin biopsy. No phosphorylated  $\alpha$ -synuclein was detected in controls. Patients with MSA had greater phosphorylated  $\alpha$ -synuclein deposition ( $p < 0.0001$ ) and more widespread peripheral distribution ( $p < 0.0001$ ) than patients with PD. These results provided >90% sensitivity and specificity in distinguishing between the 2 disorders.

### Discussion

$\alpha$ -synuclein is present in the peripheral autonomic nerves of patients with MSA and when combined with synuclein distribution accurately distinguishes MSA from PD.

### Classification of Evidence

This study provides Class II evidence that measurement of phosphorylated  $\alpha$ -synuclein in skin biopsies can differentiate patients with MSA from those with PD.

## RELATED ARTICLE

### Editorial

On the Track of  $\alpha$ -Synuclein in the Body: Skin Biopsies for Diagnosing Synucleinopathies?  
Page 691

## MORE ONLINE

### Class of Evidence

Criteria for rating therapeutic and diagnostic studies

[NPublic.org/coe](https://npublications.org/coe)

### CME Course

[NPublic.org/cmelist](https://npublications.org/cmelist)

\*These authors contributed equally to this work as first authors.

From the Department of Neurology (C.G., N.W., R.F.), Beth Israel Deaconess Medical Center, Boston, MA; Department of Pathology (S.R.), NIH, Bethesda, MD; Department of Neurology (D.K.), University of Colorado, Aurora, CO; and Department of Neurology (J.-A.P., H.K.), NYU Grossman School of Medicine, New York, NY.

Go to [Neurology.org/N](https://Neurology.org/N) for full disclosures. Funding information and disclosures deemed relevant by the authors, if any, are provided at the end of the article.

## Glossary

**AUC** = area under the curve; **BIDMC** = Beth Israel Deaconess Medical Center; **IENFD** = intraepidermal nerve fiber density; **MDS-UPDRS** = Movement Disorders Society Unified Parkinson's Disease Rating Scale; **MSA** = multiple system atrophy; **NYU** = New York University; **OHQ** = Orthostatic Hypotension Questionnaire; **P-SYN** = phosphorylated  $\alpha$ -synuclein; **PD** = Parkinson disease; **RBD** = REM sleep behavior disorder; **ROC** = receiver operating characteristic; **UMSARS** = Unified Multiple System Atrophy Rating Scale; **UPSIT** = University of Pennsylvania Smell Identification Test.

Multiple system atrophy (MSA) is a rapidly progressive neurodegenerative disorder characterized by the presence of autonomic dysfunction and motor features such as parkinsonism and/or cerebellar ataxia.<sup>1,2</sup> The pathologic hallmark of MSA is the presence of misfolded phosphorylated  $\alpha$ -synuclein (P-SYN) predominantly within glial cytoplasmic inclusions, thus classifying MSA as an oligodendroglial  $\alpha$ -synucleinopathy.<sup>2</sup> The pathophysiologic mechanisms linking  $\alpha$ -synuclein deposition to neurodegeneration in the  $\alpha$ -synucleinopathies are not fully characterized.<sup>3</sup>

An unmet need exists for an accurate diagnostic biomarker for  $\alpha$ -synucleinopathies. Autopsy studies of patients with MSA and Parkinson disease (PD) show a high misdiagnosis rate, particularly early in the disease course. This diagnostic inaccuracy has important implications for patient care, patient life planning, and therapeutic trials. An emerging diagnostic biomarker for synucleinopathies is the identification of  $\alpha$ -synuclein in tissues and organs outside the CNS. Peripheral deposition of  $\alpha$ -synuclein has been identified within cutaneous autonomic nerve fibers seen on skin biopsy tissue<sup>4,6</sup> and reports that P-SYN is detected in patients with PD, REM sleep behavior disorder (RBD), Lewy body dementia, pure autonomic failure, and MSA,<sup>4,6,7</sup> have led to a growing interest in the use of this technique as a diagnostic biomarker for the synucleinopathies.<sup>8-10</sup> Intriguingly, several studies have reported cutaneous deposition of phosphorylated  $\alpha$ -synuclein in MSA, despite this disorder being traditionally classified as a CNS-predominant synucleinopathy. These studies suggest that the distribution of the deposition in MSA may have unique pathologic features compared with the other synucleinopathies.<sup>8,9,11</sup>

We hypothesized that the cutaneous  $\alpha$ -synuclein distribution pattern coupled with the assessment of intraepidermal sensory nerve fiber density and dermal autonomic nerve fiber density would provide a unique pathologic signature in MSA that combined with select clinical features could prove a specific diagnostic biomarker for MSA. To test this hypothesis, we determined the topography of cutaneous  $\alpha$ -synuclein deposition in samples obtained from patients with MSA and compared it with the cutaneous  $\alpha$ -synuclein deposition pattern in patients with PD and healthy controls. We also investigated whether clinical features, combined with a pathologic signature of phosphorylated  $\alpha$ -synuclein distribution, aided in distinguishing MSA from PD.

## Methods

### Design and Recruitment

This was a prospective single-visit cohort study of 3 different groups: (1) individuals with MSA, (2) PD, and (3) healthy controls. Patients with MSA and PD were recruited by the autonomic and movement disorders groups at the Neurology Departments of the Beth Israel Deaconess Medical Center (BIDMC), New York University (NYU) and University of Colorado were recruited for study participation from 2016 to 2021. Healthy control subjects were recruited by local advertisement. Patients with MSA were included if they met the criteria for probable MSA using current diagnostic criteria for MSA.<sup>12</sup> Patients with PD were included if they met the criteria for definite PD using the UKPDS brain bank criteria with 3 or more supportive features including diagnosis >5 years and excellent levodopa response.<sup>13</sup> Exclusion criteria for MSA and PD followed diagnostic guidelines.<sup>12,13</sup> Other exclusion criteria included anticoagulation use, other underlying disorder that could cause a neuropathy, or risks of complication to a skin biopsy (e.g., allergy to lidocaine). Controls were included if they had no known medical conditions. Exclusion criteria for healthy controls included a family history of synucleinopathy, clinical features of neuropathy, or a history suggestive of RBD.

### Standard Protocol Approvals, Registrations, and Patient Consents

The study was approved by the 3 institutional review boards (BIDMC: 2015P000433; NYU: i08-1408\_CR12; Colorado: COMIRB 12-0705). Written informed consent was obtained from all participants.

### Examination and Clinical Testing

All participants underwent a general history and detailed neurologic examination. MSA disease severity was rated by the Unified Multiple System Atrophy Rating Scale (UMSARS),<sup>14</sup> whereas PD severity was rated by the Movement Disorders Society Unified Parkinson's Disease Rating Scale (MDS-UPDRS).<sup>15</sup> Both disorders were also rated with the Hoehn and Yahr scale.<sup>16</sup> Most participants completed the University of Pennsylvania Smell Identification Test (UPSIT),<sup>17</sup> and all completed the Montreal Cognitive Assessment.<sup>18</sup> All participants completed orthostatic blood pressures in the supine resting position and after 3 minutes of standing. All testing and examinations were completed in the OFF state for medications used to treat motor symptoms (e.g., levodopa and dopaminergic agonists) and for the

symptomatic treatment of orthostatic hypotension (e.g., midodrine and droxidopa).

### Questionnaires

Participants completed the orthostatic hypotension questionnaire,<sup>19</sup> the single-question REM sleep behavioral disorder questionnaire,<sup>20</sup> the MSA red flags questionnaire,<sup>21</sup> and the Parkinson disease questionnaire.<sup>22</sup>

### Autonomic Function Testing

Cardiovascular parasympathetic function testing (the heart rate response to deep respiration and the Valsalva maneuver) and cardiovascular sympathetic function (the blood pressure response to a Valsalva maneuver and tilt-table testing to 60° for 10 minutes) was performed in patients from BIDMC and NYU. Continuous ECG monitoring, continuous beat-to-beat blood pressure recordings, and manual blood pressure measurements every minute during tilt-table testing were recorded.

### Pathologic Evaluation

Three-millimeter punch skin biopsies were obtained from the lateral distal thigh (20 cm above the lateral knee), proximal thigh (20 cm below the lateral hip), and posterior cervical region (2 cm lateral to the C7 spinous process) after local anesthesia with 2% lidocaine. Skin biopsy specimens were fixed in Zamboni solution for 18 hours and cryoprotected overnight (20% glycerol and 20% 0.4 M Sorensen buffer). Tissue blocks were cut by freezing microtome into 50- $\mu$ m-thick sections. An average of 12 tissue sections were analyzed per biopsy with different immunostaining combinations. Additional sections were analyzed in cases in which sweat glands or arrector pili muscles were not identified within the original sections. Pathologic evaluation of specimens was completed by 2 authors (C.H.G. and N.W.).

### Immunohistochemistry

Double-labeled immunofluorescent staining was performed using our previously published methods for covisualizing total nerve fibers and  $\alpha$ -synuclein-positive nerve fibers.<sup>4</sup> The primary antibodies used to visualize total nerve fibers included the pan-axonal marker protein gene product 9.5 (PGP 9.5, rabbit polyclonal, UltraClone, RA95101; 1:10,000 or PGP 9.5, mouse monoclonal, RA9503; Ultraclone; 1:1,000), the polyclonal antibody targeting total  $\alpha$ -synuclein recognized multiple binding sites from amino acids 111–131<sup>23</sup> (rabbit polyclonal, AB5038P, Chemicon 1:13,000), and antibody targeting phosphorylated  $\alpha$ -synuclein (mouse monoclonal, Covance, New Jersey, MMS-5091, 1:500).<sup>4</sup> Dual immunostaining with PGP 9.5 and phosphorylated or PGP 9.5 and total  $\alpha$ -synuclein was performed for all samples as previously reported.

### Confocal Imaging

All the stained sections were initially examined under a fluorescent microscope, with areas of interest imaged by confocal

microscopy (Zeiss LSM5 Pascal Exciter; Carl Zeiss, Thornwood, NY). A series of images of optical sections were acquired at 3- $\mu$ m intervals throughout the depth of the 50- $\mu$ m section as a z-stack (Carl Zeiss, Lens Plan-Apochromat x20/0.8). The confocal scan condition was set based on the optimal ratio of signal intensity to noise for the nerve fibers stained with different primary antibodies of slides from control subjects; then, the confocal parameters for scanning were fixed in all slides scanned.

### Quantification of Nerve Fiber Density

#### *Intraepidermal Nerve Fiber Density*

Biopsies underwent blinded intraepidermal nerve fiber density (IENFD) counting with PGP9.5-positive fibers, and results were expressed as number of fibers crossing the dermal-epidermal junction per millimeter as previously described.<sup>24</sup>

#### *Sweat Gland Nerve Fiber Density*

Sweat glands were imaged, and nerve fiber densities were quantified using our previously described technique.<sup>25</sup> Briefly, 30- $\mu$ m deep Z-stack composite confocal images were created for each sweat gland, and the gland was highlighted as the area of interest. PGP9.5 innervated fibers were detected within the area of interest, and expressed as the ratio of fibers to total gland area. Sweat gland innervation was evaluated in a blinded fashion.

#### *Pilomotor Nerve Fiber Density*

Pilomotor muscles were imaged, and nerve fiber densities were quantified as previously published.<sup>26</sup> The average number of nerve fibers intersecting 5 horizontal lines across the width of the pilomotor muscle in 3- $\mu$ m-thick confocal images was reported in fiber/mm.

#### *Phosphorylated $\alpha$ -Synuclein Quantitation*

Slides were deidentified, and all slide readers were blinded to study participant diagnosis. Phosphorylated  $\alpha$ -synuclein-positive fibers were required to be completely colocalized within PGP9.5-positive nerve fibers by review of Z-stack image analysis (i.e., areas of synuclein that did not colocalize were defined as artifact). The number of positive results was noted for each cutaneous dermal structure for each tissue section for each biopsy. For example, if one or more synuclein-positive fibers were found to innervate a single pilomotor muscle, the pilomotor muscle is defined as one synuclein-positive structure. A second, separate pilomotor muscle with one or more synuclein-positive fibers would count as a 2nd P-SYN-positive structure. A quantitative analysis of phosphorylated  $\alpha$ -synuclein was performed for each patient. Results were expressed as the number of P-SYN-positive structures. The location of P-SYN deposition was calculated across the various biopsies using a distribution coefficient at the posterior cervical, proximal thigh, and distal

thigh. The calculation of the distribution coefficient (DC) = (PC<sub>score</sub> - DT<sub>score</sub>)/(PC<sub>score</sub> + PT<sub>score</sub> + DT<sub>score</sub>) where the posterior cervical (PC), proximal thigh (PT), and distal thigh (DT) scores are the quantitative analysis of synuclein deposition at each biopsy site. Scores with zero in the numerator were assigned a score of zero. The scores ranged from (+)1 (indicating that P-SYN was located only at the posterior cervical site only) to (-)1 (indicating that P-SYN was located at only the distal thigh site) and indicated the relative distribution of P-SYN from a proximal to distal gradient.

### Statistical Analysis

Statistical data analysis was performed using SPSS v17.0 (IBM, Chicago, IL). Data are presented as mean ± SD. Group differences in total nerve fiber density, total α-synuclein ratio, phosphorylated α-synuclein deposition, and autonomic test results are reported. Differences between groups were analyzed by ANOVA with the Holm-Sidak post hoc test when normally distributed (Shapiro-Wilk). If data were not normally distributed, the Kruskal-Wallis with Dunn method for post hoc analysis was used. The sensitivity and specificity were calculated for each individual test and in combinations to identify optimal combinations of tests to distinguish PD vs MSA using receiver operating characteristic (ROC) curves. Cutoff thresholds for the ROC were selected by the highest product of sensitivity × specificity with an edge toward specificity in situations where equivalent results for 2 values were obtained. An exploratory analysis of a combination of ROC curve results was included using an AND operator where both results above the preselected ROC threshold were positive, but if either or both were below the ROC threshold,

the result was negative. Discrimination between groups using ROC curves is reported as the area under the curve (AUC). Associations between α-synuclein deposition, autonomic test results, and examination scores are expressed as Pearson correlations.

## Results

### Demographics

Thirty-one patients with MSA (15 men and 16 women; mean age 61 ± 9 years; body mass index of 30.7 ± 2.4 kg/m<sup>2</sup>; 17 had MSA-C and 14 had MSA-P), 54 patients with PD (30 men and 24 women; mean age 64 ± 8 years; body mass index of 29.2 ± 2.6 kg/m<sup>2</sup>), and 24 healthy controls (12 men and 12 women; mean age 62 ± 8 years; body mass index of 31.9 ± 3.1 kg/m<sup>2</sup>) participated in this study. Table 1 summarizes the participant's demographic information and their disease-specific scores.

### Autonomic Function Tests

All participants completed orthostatic vital signs, and 22 patients with MSA completed heart rate variability to paced breathing and a Valsalva maneuver. All individuals with PD and control subjects completed testing. Table 2 summarizes the autonomic function testing results. As expected, autonomic abnormalities were more severe in the MSA group.

### Sensory and Autonomic Nerve Fiber Densities

In patients with MSA, intraepidermal nerve fiber densities, a measure of small sensory afferents, were similar to controls at all biopsy sites. In contrast, patients with PD had lower nerve

**Table 1** Demographic Characteristics of Participants

	MSA (N = 31)	PD (N = 54)	Control (N = 24)	p Value (ANOVA)
<b>Sex</b>	16 F, 15 M	24 F, 30 M	12 F, 12 M	0.47 <sup>a</sup>
<b>Age</b>	61 ± 9	64 ± 8	62 ± 8	0.80
<b>BMI</b>	29.7 ± 2.6	29.2 ± 2.8	30.9 ± 2.6	0.20
<b>Duration of disease</b>	3.4 ± 2.7	4.9 ± 4.2 <sup>b</sup>	NA	<0.0001
<b>Disease-specific rating scales</b>	UMSARS-1: 21.8 ± 7.7 Range (11–44) UMSARS-2: 21.6 ± 8.7 Range (9–43)	MDS-UPDRS total: 49.0 ± 20.2 Range (15–90) MDS-UPDRS -3: 33.4 ± 13.8 Range (7–68)	NA	NA
<b>Hoehn and Yahr</b>	2.6 ± 0.9 Range (1–4)	2.1 ± 0.5 Range (1–4)	0 ± 0	0.021 <sup>b</sup>
<b>MOCA</b>	25.7 ± 2.7	26.2 ± 2.2	25.9 ± 3.4	0.42
<b>UPSIT</b>	N = 22 32.9 ± 5.6	N = 54 23.4 ± 5.5 <sup>b</sup>	N = 24 35.8 ± 2.1 <sup>c</sup>	<0.0001 (KW)

Abbreviations: KW = Kruskal-Wallis used instead of ANOVA because data not normally distributed; MSA = multiple system atrophy; MOCA = Montreal Cognitive Assessment; NS = not significant; NA = not available; PD = Parkinson disease; UPSIT = University of Pennsylvania Smell Identification Test.

<sup>a</sup> Calculated using a 2 × 3 Fisher exact test.

<sup>b</sup> p < 0.01 PD vs MSA.

<sup>c</sup> p < 0.01 control vs PD.



**Table 2** Autonomic Function Testing

Test	MSA (N = 31)	PD (N = 54)	Control (N = 24)	ANOVA <i>p</i> value
Supine SBP (mm Hg)	152 ± 18	136 ± 17 <sup>a</sup>	127 ± 6 <sup>b,c</sup>	<0.0001 (KW)
Supine DBP (mm Hg)	89 ± 7	82 ± 5 <sup>a</sup>	78 ± 3 <sup>b</sup>	<0.0001 (KW)
Supine HR (beats/min)	81 ± 12	64 ± 7 <sup>a</sup>	69 ± 11 <sup>b,c</sup>	<0.0001 (KW)
Upright tilt SBP (mm Hg)	117 ± 23	120 ± 17	122 ± 8 <sup>b,c</sup>	0.27
Upright tilt DBP (mm Hg)	74 ± 6	76 ± 5	80 ± 3 <sup>b,c</sup>	<0.0001 (KW)
Upright tilt HR (beats/min)	87 ± 9	69 ± 7	76 ± 12 <sup>b,c</sup>	<0.0001 (KW)
Fall in SBP on tilt (mm Hg)	42 ± 18	15 ± 6 <sup>a</sup>	5 ± 6 <sup>b,c</sup>	<0.0001 (KW)
	MSA (N = 22)	PD (N = 54)	Control (N = 24)	
Expiratory to inspiratory ratio	1.12 ± 0.06	1.19 ± 0.11 <sup>a</sup>	1.32 ± 0.11 <sup>b,c</sup>	<0.0001
Valsalva ratio	1.24 ± 0.13	1.34 ± 0.19 <sup>a</sup>	1.43 ± 0.11 <sup>b,c</sup>	<0.0001
Valsalva phase 2 systolic blood pressure drop (mm Hg)	-55 ± 29	-42 ± 13 <sup>a</sup>	-36 ± 18 <sup>b</sup>	<0.0001
Valsalva phase 4 systolic blood pressure overshoot (mm Hg)	1 ± 9	10 ± 10 <sup>a</sup>	26 ± 11 <sup>b,c</sup>	<0.0001

Abbreviations: DBP = diastolic blood pressure; HR = heart rate; KW = Kruskal-Wallis used instead of ANOVA because data not normally distributed; MSA = multiple system atrophy; PD = Parkinson disease; SBP = systolic blood pressure.

<sup>a</sup> *p* < 0.01 PD vs MSA.

<sup>b</sup> *p* < 0.01 control vs MSA.

<sup>c</sup> *p* < 0.01 control vs PD.

densities at both the distal thigh and the proximal thigh than patients with MSA and controls (Table 3). Pilomotor nerve fiber densities, a measure of sympathetic innervation of smooth muscle, were similar in MSA and controls at all sites but were reduced in patients with PD at the distal thigh and proximal thigh sites (Table 3). Although differences in ANOVA between groups were noted in sweat gland nerve fiber density, a measure of sympathetic sudomotor cholinergic innervation, there were no differences in post hoc testing between groups at any biopsy site.

### Phosphorylated $\alpha$ -Synuclein

Phosphorylated  $\alpha$ -synuclein was detected within at least one biopsy in all the patients with MSA, in 94% (51/54) of patients with PD, and in none of the control subjects as reported in Table 3. Of note, the 3 patients with PD who did not have P-SYN present on skin biopsy did not have evidence of REM sleep behavior disorder. Phosphorylated  $\alpha$ -synuclein was deposited within sudomotor nerve fibers, pilomotor nerve fibers, vasomotor nerve fibers, nerve bundles, and the subepidermal plexus (Figure 1). There was no phosphorylated  $\alpha$ -synuclein detected within nociceptive sensory fibers (intraepidermal fibers). The quantitative analysis of phosphorylated  $\alpha$ -synuclein revealed significantly higher levels in patients with MSA compared with PD (*p* < 0.0001 for all biopsy sites; Figure 1, Table 3).

The topography of phosphorylated  $\alpha$ -synuclein deposition differed between patients with MSA and PD. The deposition of phosphorylated  $\alpha$ -synuclein in patients with PD followed a proximal-distal gradient, with the posterior cervical site

positive in 93% of cases, the proximal thigh positive in 33% of cases, and the distal thigh in 17% of cases. In contrast, deposition of  $\alpha$ -synuclein in patients with MSA appeared more evenly distributed: the posterior cervical was positive in 84% of cases, the proximal thigh in 87% of cases, and the distal thigh in 77% of cases. The topographic distribution was calculated using the distribution coefficient for P-SYN. In PD, the distribution coefficient was  $0.64 \pm 0.48$  (indicating a posterior cervical predilection), whereas the distribution for MSA was  $0.07 \pm 0.37$  (indicating a more even distribution across all biopsy sites) (*p* < 0.0001 PD vs MSA). This topographical distribution and quantity of P-SYN deposition is seen visually in Figure 2.

In addition, the specific location of phosphorylated  $\alpha$ -synuclein deposition within a given biopsy differed between patients with MSA and PD: In patients with MSA, P-SYN was detected in the subepidermal plexus region (composed of sensory afferent fibers) in 68% of cases (21/31) and only in 6% of patients with PD (3/54).

### Relationship Between $\alpha$ -Synuclein Deposition, Neurologic Examination, and Autonomic Function

In patients with MSA, UMSARS scores were higher in those with greater P-SYN deposition (*R* = 0.632, *p* = 0.001); however, there was no correlation between the MDS-UPDRS and P-SYN deposition in patients with PD (*R* = 0.2, *p* = 0.14). In the combined MSA and PD groups, higher Hohn and Yahr scores were associated with greater P-SYN deposition (*R* = 0.41, *p* < 0.0001).

**Table 3** Pathologic Quantitation of Nerve Fiber Density and Synuclein Deposition

Test	MSA (N = 31)	PD (N = 54)	Control (N = 24)	ANOVA	AUC	95% CI for the AUC	AUC <i>p</i> value
IENFD distal thigh	10.2 ± 2.4 <sup>b</sup>	4.6 ± 2.5	12.9 ± 2.1 <sup>b</sup>	<i>p</i> < 0.0001	0.916	0.872–0.965	<0.0001
IENFD proximal thigh	14.6 ± 3.2 <sup>a</sup>	9.4 ± 4.1	15.3 ± 5.4 <sup>a</sup>	<i>p</i> < 0.0001	0.893	0.823–0.963	<0.0001
IENFD posterior cervical	30.8 ± 6.2 <sup>a</sup>	24.9 ± 5.0	27.1 ± 5.9	<i>p</i> < 0.0001	0.821	0.733–0.907	<0.0001
PMNFD distal thigh	53.4 ± 18.5 <sup>a</sup>	42.3 ± 13.3	55.4 ± 10.9	<i>p</i> < 0.0001	0.594	0.467–0.723	0.16
PMNFD proximal thigh	62.3 ± 13.4 <sup>a</sup>	53.1 ± 16.1	65.1 ± 14.3	<i>p</i> < 0.0001	0.433	0.294–0.570	0.36
PMNFD posterior cervical	78.7 ± 19.3 <sup>a</sup>	65.4 ± 22.5	76.2 ± 16.5	<i>p</i> = 0.042	0.412	0.282–0.541	0.23
SGNFD distal thigh	0.11 ± 0.05	0.09 ± 0.05	0.12 ± 0.04	<i>p</i> = 0.011	0.619	0.489–0.750	0.0.07
SGNFD proximal thigh	0.14 ± 0.06	0.13 ± 0.05	0.15 ± 0.06	<i>p</i> = 0.014	0.553	0.417–0.689	0.44
SGNFD posterior cervical	0.18 ± 0.07	0.17 ± 0.07	0.18 ± 0.06	<i>p</i> = 0.16	0.458	0.324–0.592	0.54
P-SYN distal thigh	4.7 ± 3.6 <sup>b</sup>	0.4 ± 0.9	0 ± 0	<i>p</i> < 0.0001	0.873	0.790–0.957	<0.0001
P-SYN proximal thigh	4.8 ± 3.4 <sup>b</sup>	0.9 ± 1.2	0 ± 0	<i>p</i> < 0.0001	0.839	0.739–0.939	<0.0001
P-SYN posterior cervical	5.5 ± 3.6 <sup>b</sup>	2.0 ± 1.2	0 ± 0	<i>p</i> < 0.0001	0.792	0.665–0.917	<0.0001
P-SYN total	15.0 ± 6.1	3.2 ± 1.9	0 ± 0	<i>p</i> < 0.0001	0.983	0.954–1.01	<0.0001
P-SYN distribution coefficient	0.07 ± 0.37 <sup>b</sup>	0.64 ± 0.48	N/A	N/A	0.825	0.740–0.910	<0.0001

Abbreviations: AUC = area under the curve; IENFD = intraepidermal nerve fiber density; MSA = multiple system atrophy; N/A = not applicable; P-SYN = phosphorylated  $\alpha$ -synuclein; PMNFD = pilomotor nerve fiber density; SGNFD = sweat gland nerve fiber density.

<sup>a</sup>*p* < 0.05 vs PD with Holm-Sidak post hoc testing.

<sup>b</sup>*p* < 0.01 vs PD PD with Holm-Sidak post hoc testing. Accuracy of PD vs MSA: a measure of the area under the ROC curve analysis in PD and MSA. NA: no synuclein detected therefore distribution not calculated. AUC: area under the curve from the ROC analysis. 95% CI for the AUC: the 95% CI derived from the ROC curve analysis.

There were correlations in the combined MSA and PD groups with phosphorylated  $\alpha$ -synuclein levels and autonomic dysfunction as measured by decreased heart rate variability to paced breathing ( $R = -0.29$ ,  $p = 0.008$ ), reduced heart rate response to a Valsalva maneuver ( $R = -0.43$ ,  $p < 0.0001$ ), the fall in blood pressure during phase 2 of the Valsalva maneuver ( $R = -0.26$ ,  $p = 0.017$ ), and reduced blood pressure overshoot in response to a Valsalva maneuver ( $R = -0.58$ ,  $p < 0.0001$ ). There were correlations between P-SYN deposition and supine systolic blood pressure ( $R = 0.42$ ,  $p < 0.0001$ ), supine diastolic blood pressure ( $R = 0.43$ ,  $p < 0.0001$ ), supine heart rate ( $R = 0.58$ ,  $p < 0.0001$ ), and fall in systolic blood pressure on the upright tilt-table test ( $R = -0.47$ ,  $p < 0.0001$ ).

### Sensitivity and Specificity to Distinguish MSA From PD

The sensitivity and specificity of any given measure to distinguish MSA from PD were calculated using ROC curves, and the discrimination between groups (area under the ROC curve) is reported in Table 3 and Figure 3. The metrics that best distinguished MSA from PD include (1) the quantitation of P-SYN across all 3 biopsy sites (a sensitivity of 96.8% and a specificity of 94.4%, with a P-SYN threshold of  $\geq 7.0$  and an AUC of 0.983) and (2) the distribution coefficient of P-SYN (sensitivity 77% and specificity 74%, with a distribution coefficient threshold of  $<0.5$  with an AUC of 0.826). Combining cutoff thresholds of P-SYN total  $\geq 7.0$  and the distribution

coefficient  $\leq 0.5$  provides 96.8% sensitivity and 98.1% specificity at distinguishing MSA from PD. The results are displayed in a confusion matrix format in eTables 1 and 2, links. [www.com/WNL/C608](http://www.com/WNL/C608). Other pathologic combinations offered similar results. For example, the quantitation of P-SYN across all 3 biopsy sites (with a P-SYN threshold of 7.0) combined with the IENFD at the distal thigh (with an IENFD threshold of 7.95 fibers/mm) provided a  $>94\%$  sensitivity and specificity at distinguishing PD from MSA.

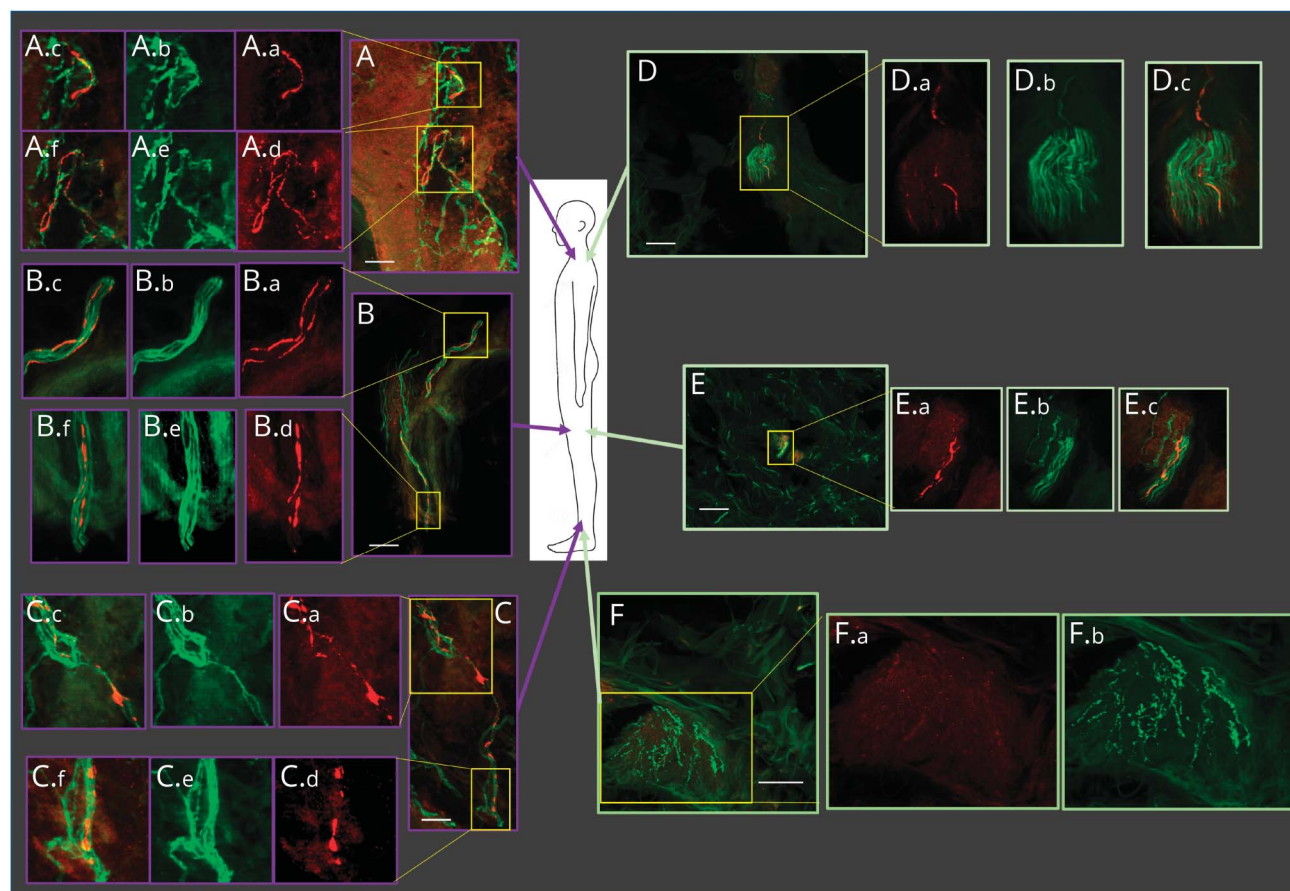
### Classification of Evidence

The primary question in this study was to determine whether skin biopsies with quantitation of phosphorylated  $\alpha$ -synuclein and IENFD biopsy could differentiate MSA from PD. Patients with MSA and PD were recruited using standard clinical diagnostic criteria. The diagnostic test result and clinical status were defined by different individuals. This study provides Class II evidence that measurement of phosphorylated  $\alpha$ -synuclein in skin biopsies can differentiate patients with MSA from those with PD.

### Discussion

This prospective cohort study demonstrates that patients with MSA can be differentiated from those with PD and healthy controls with excellent sensitivity and specificity using cutaneous neuropathologic assessments combined with selected clinical features. Specifically, the study shows that (1)

**Figure 1** Distribution of Phosphorylated  $\alpha$ -Synuclein in Parkinson Disease (PD) and Multiple System Atrophy (MSA)



Biopsy locations are shown in the middle cartoon figure. Biopsies from a representative patient with MSA are shown in purple outlined boxes (A, B, C), and a patient with PD in green outlined boxes (D, E, F). The posterior cervical region biopsy of the patient with MSA, shown in panel A (A.a–A.f) reveals multiple  $\alpha$ -synuclein positive regions in the sub-epidermal plexus. These positive regions are shown in expanded detail in A.a–A.c and A.d–A.f; phosphorylated  $\alpha$ -synuclein in red (A.a and A.d), the overlying nerve fibers stained with PGP9.5 in green (A.b and A.e), and merged images in A.c and A.f. Similar images are seen in the proximal thigh (B) and distal thigh (C) biopsy sites. The biopsy from the posterior cervical region of a representative patient with PD, shown in panel D, reveals two adjacent positive fibers. The positive regions are shown in expanded detail in the yellow outlined box; phosphorylated  $\alpha$ -synuclein in red in D.a, the overlying nerve fibers stained with PGP9.5 in green in D.b, and the merged image in D.c. A similar result is shown in the proximal thigh (E) with a single fiber containing phosphorylated  $\alpha$ -synuclein in E.a, the overlying nerve fibers stained with PGP 9.5 in green in E.b., and the merged image in E.c. The biopsy sites at the distal thigh (F) demonstrate regions where no phosphorylated  $\alpha$ -synuclein is observed (F.a.), although nerve fibers stained with PGP9.5 are clearly identified (F.b.). White scale bar = 5  $\mu$ m.

phosphorylated  $\alpha$ -synuclein is present within cutaneous autonomic nerve fibers in patients with MSA and PD but not in healthy age-matched controls; (2) cutaneous phosphorylated  $\alpha$ -synuclein deposition is greater in patients with MSA compared with patients with PD; (3) the topographic distribution of  $\alpha$ -synuclein deposition differs in patients with MSA vs PD, namely, patients with PD showed a proximal to distal gradient, whereas deposition was more evenly distributed in patients with MSA; and (4) patients with PD have a mild length-dependent sensory and autonomic neuropathy that is not present in patients with MSA. Collectively, these data suggest that skin biopsy may be an accurate method to pathologically confirm a diagnosis of a synucleinopathy and distinguish between MSA and PD.

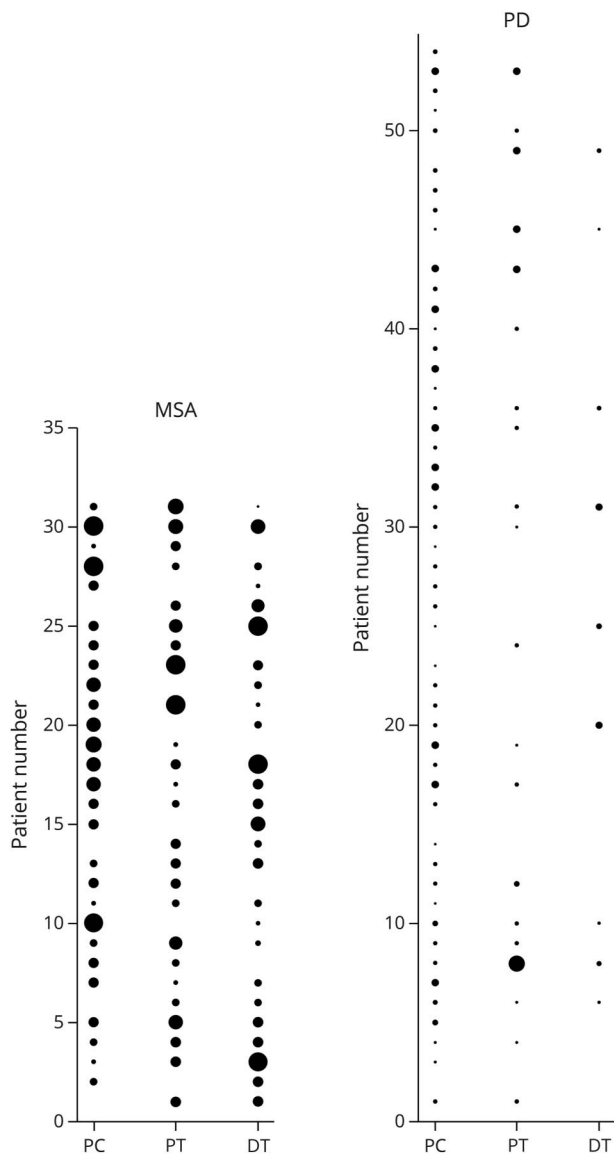
There is a need for improved diagnostic accuracy in synucleinopathies. Recent autopsy studies in MSA reported a diagnostic accuracy of 62% and 78%.<sup>27,28</sup> A similar diagnostic accuracy has been reported in autopsy studies of PD; a summary of 3 autopsy

studies of patients with early PD suggests a diagnostic accuracy of only 58%.<sup>29,30</sup> The response to pharmacotherapy, need for ancillary support, quality of life, and rate of progression differs markedly between these disorders. These factors, when coupled with diagnostic inaccuracy, have implications for patient care, therapeutic interventions including clinical trials, prognostication, and planning for patients and their families. Recent refinements to the diagnostic criteria for MSA<sup>31</sup> and PD<sup>32</sup> should result in improved diagnostic accuracy; however, the new criteria are unlikely to fully remediate the diagnostic inaccuracy.

Consistent with other studies,<sup>11</sup> we show that the topographic distribution of P-SYN differs in PD compared with MSA.<sup>33</sup> We have leveraged this difference to develop a distribution index that enhances the diagnostic discrimination of the test. Our findings are supported by other studies that show differences in the peripheral distribution of P-SYN in patients with MSA.<sup>11</sup> It is not surprising that topographic differences



**Figure 2** Topographical Distribution of P-SYN Across Study Subjects



The relative amount of synuclein deposition by biopsy site is shown for each individual subject; the larger the circle, the greater the synuclein deposition. The left panel is for subjects with MSA, and the right panel is for individuals with PD. When comparing the 2 panels, P-SYN deposition is greater and more evenly distributed than in MSA than in PD. DT = distal thigh; PC = posterior cervical; PT = proximal thigh.

exist between these 2 synucleinopathies given the differences in their respective CNS pathologies. MSA is characterized by widespread  $\alpha$ -synuclein–positive glial cytoplasmic inclusions and associated neurodegeneration of striatonigral and olivopontocerebellar pathways, whereas PD neuropathology is characterized by neural inclusions in the form of Lewy bodies and Lewy neurites, with cell loss in the substantia nigra. The mechanisms that underlie the PNS distribution differences are not known. Nonetheless, the unique deposition pattern of phosphorylated  $\alpha$ -synuclein seen in MSA provides a powerful tool to discriminate MSA from PD. It should also be noted that several potential other pathologic signatures (such as

reduced IENFD or pilomotor nerve fiber density) could have been included in the final model with equally effective discriminatory power. As noted in the eTables, only 2 patients were misclassified. The addition of other variables would not have modified those results and does suggest that the model has achieved optimal accuracy in providing a unique pathologic signature to discriminate between the 2 disorders in this data set. Future studies with expanded numbers of subjects could investigate the role of the inclusion of clinical data in the model (such as anosmia, UPSIT, orthostatic hypotension, and heart rate response to orthostatic change).

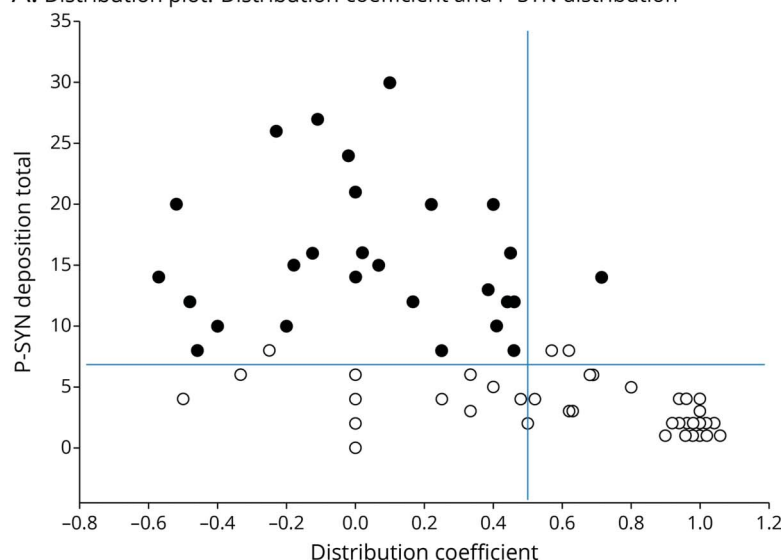
Our cutaneous pathologic findings (decreased autonomic and small fiber sensory innervation in PD compared with MSA) are consistent with prior reports of peripheral nerve degeneration in Parkinson disease and reduced orthostatic heart rate response.<sup>34,35</sup> However, there is discordance between these findings and the observed amount and distribution of  $\alpha$ -synuclein deposition. This observation highlights that the basis of these established phenotypic differences and the mechanism whereby  $\alpha$ -synuclein causes neurodegeneration are not fully established. Possibilities to explain the phenotypic differences between the 2 disorders include (1) differences at a cellular level, for example, the recent identification of P-SYN in Schwann cells of patients with MSA but not the Lewy body diseases,<sup>33</sup> and (2) differences at a molecular level, that is, the different conformational changes in  $\alpha$ -synuclein in the Lewy body disorders and MSA that have been observed in several studies.<sup>36,37</sup> Our data do not provide a full explanation for the pathologic and clinical phenotypic differences among the synucleinopathies. Our study was not designed to directly address this question but does add to the information that surrounds the different distributions of central and peripheral nervous system  $\alpha$ -synuclein deposition in MSA and PD.

The detection and differential distribution of  $\alpha$ -synuclein in MSA and PD highlight the questions as to how and when  $\alpha$ -synuclein is deposited in the cutaneous nerves and what is the topography of peripheral spread over time. Specifically, how does cutaneous  $\alpha$ -synuclein fit into the Braak staging system,<sup>38</sup> which hypothesizes that Lewy pathology starts in the olfactory bulb and enteric nervous system, and invades the brain via the vagus nerve and possibly via a sympathetic spreading route that includes the sympathetic trunk and heart.<sup>39</sup> A recent study has proposed the existence of 2 parkinsonian subtypes.<sup>40</sup> One described as bottom-up or body first and characterized by origin in the peripheral autonomic nervous system and ascent via the vagus and sympathetic autonomic nerves. This subtype is characterized by the occurrence of RBD prior to the onset of motor features. The second subtype, top-down or brain first, is characterized by origin in the brain or olfactory tubercle with downward spread via the brainstem. In this subtype, RBD occurs after the appearance of motor features. Our study is not powered to assess the relationship of RBD to the amount and distribution

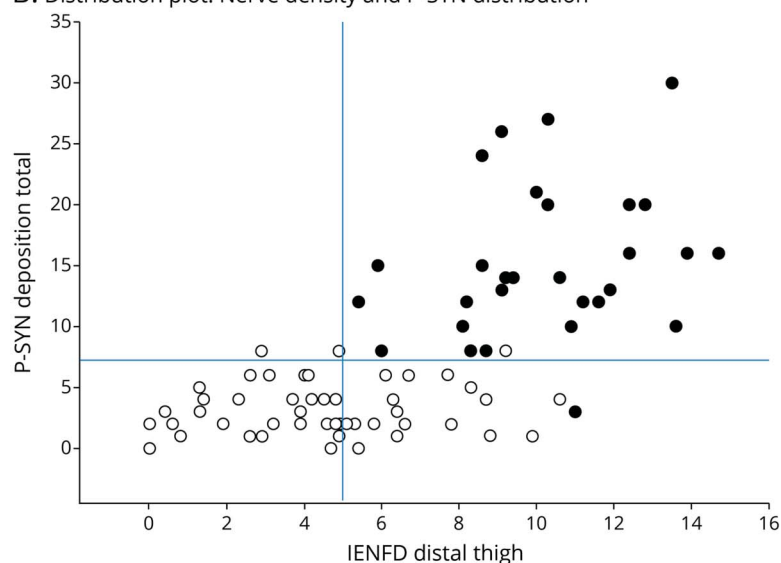


**Figure 3** Test Characteristics That Distinguish Multiple System Atrophy (MSA) From Parkinson Disease (PD)

**A.** Distribution plot: Distribution coefficient and P-SYN distribution



**B.** Distribution plot: Nerve density and P-SYN distribution



The plots of phosphorylated  $\alpha$ -synuclein are shown for patients with MSA (black circles) and PD (open circles). In Figure 1A, the plot of phosphorylated against the synuclein distribution coefficient is shown. In Figure 1B, the plot of phosphorylated against the intraepidermal nerve fiber density (IENFD) is shown. In both graphs, the cutoff thresholds identified using ROC curves are shown (see eTable 1, [www.com/WNL/C608](http://www.com/WNL/C608)). In Figure 1A, the upper left quadrant indicates patients with a high probability of MSA. In Figure 1B, the upper right quadrant indicates patients with a high probability of MSA. For both graphs, all other quadrants indicate patients with PD. In both graphs, a single patient with MSA and PD is misclassified.

of  $\alpha$ -synuclein, and the cross-sectional design does not allow for assessment of the changes in distribution and deposition. These are important topics for future studies.

The results of this study provide preliminary support for the possibility that measurement of cutaneous  $\alpha$ -synuclein deposition could be used as a prognostic biomarker in PD and MSA in clinical practice, research studies, and clinical trials. The correlations between  $\alpha$ -synuclein and clinical manifestations, for example, physical examination scores, tests of autonomic function, autonomic symptoms, and anosmia are understandably modest for both patients with PD and MSA. Several factors may influence these relationships, and these have implications for the clinical use and interpretation of cutaneous  $\alpha$ -synuclein measurement as a prognostic biomarker. Factors include that most patients were

assessed and biopsied on symptomatic treatment, which may have influenced the clinical assessments. Also, the relationship between CNS  $\alpha$ -synuclein aggregation, CNS neurodegeneration, and clinical manifestations is not linear, and if cutaneous  $\alpha$ -synuclein deposition follows central deposition, similar nonlinearity would be expected. Furthermore, discordance between the rate of disease progression in MSA and PD and  $\alpha$ -synuclein deposition in the skin may influence the relationship.

In addition, the rate, extent, and distribution of cutaneous  $\alpha$ -synuclein deposition may be discontinuous with the implication that the prognostic biomarker utility of cutaneous  $\alpha$ -synuclein deposition may vary across the disease course. Further understanding of the research and clinical utility of cutaneous  $\alpha$ -synuclein measurement as a prognostic biomarker

will require longitudinal study with clinical assessments, ideally off medications and performed at multiple time points. Related questions are whether cutaneous  $\alpha$ -synuclein assessment could be used to measure target engagement of pharmacotherapy directed toward an  $\alpha$ -synuclein target and, in the long-term, could be used as a surrogate biomarker, similar to the use of the amyloid PET scan in Alzheimer disease and related disorders. These questions are of increasing importance with the growth in the number of disease-modifying therapies. Correlations were present with clinical manifestations of MSA and PD and phosphorylated  $\alpha$ -synuclein levels and total  $\alpha$ -synuclein ratios—the ratio normalizes deposition relative to nerve fiber density. Longitudinal studies and the availability of effective disease-modifying therapy will allow determination as to which of these continuous variables is the superior prognostic biomarker or measure of target engagement.

There are several limitations to this study. Other biofluid, imaging, and tissue biomarkers were not measured. At present,  $\alpha$ -synuclein biomarkers obtained from blood have tested different synuclein isoforms, including phosphorylated  $\alpha$ -synuclein, but have not yet achieved results that allow for differentiation from controls or other synucleinopathies.<sup>41</sup> In contrast, advances using real-time quaking-induced conversion (RT-QuIC) of CSF have consistently shown high sensitivity and specificity in detection of PD, with some data supporting a role in differentiating from MSA.<sup>37,42</sup> Only a single study compared RT-QuIC from CSF with skin biopsy immunofluorescent staining for P-SYN in patients with synucleinopathies and found 90% sensitivity and 100% specificity with skin biopsy phosphorylated  $\alpha$ -synulcein immunofluorescence and 78% sensitivity and 100% specificity using RT-QuIC from CSF.<sup>43</sup>

Other limitations in the present study include a relatively small sample size, where individual study subjects contribute an outsized influence on sensitivity and specificity. The results should be taken with caution until further validated. We did not include nerve fiber–specific markers (such as tyrosine hydroxylase or dopamine beta-hydroxylase) to confirm the presence of P-SYN within sympathetic adrenergic nerve fibers. Many of our participants were in the mid and late stages of the disease. The study therefore does not address the question as to how early  $\alpha$ -synuclein deposition occurs in these synucleinopathies, although a number of studies in patients with idiopathic REM sleep behavioral disorder suggest that premotor detection of phosphorylated  $\alpha$ -synuclein is expected.<sup>44-47</sup> We did not screen for some comorbid conditions such as prediabetes. The high prevalence of peripheral neuropathy in the general population due to disorders such as diabetes and impaired glucose tolerance will limit the use of nerve fiber density as a tool to discriminate between synucleinopathies. Future studies should include patients in earlier stages of the disease, followed prospectively and with neuropathologic confirmation. Not all participants in this study were able to complete a full battery of autonomic tests, and sudomotor function testing was not completed in this study.

Despite these limitations, the assessment of  $\alpha$ -synuclein deposition within the skin has the potential to provide a safe, accessible, and repeatable marker of disease pathology.

### Study Funding

This work was supported by the National Institutes of Health (NIH U54 NS065736), the Langer Family Foundation (to R.F.), the MSA Coalition (to R.F.), and the University of Colorado Skin Disease Research Center (to DSK).

### Disclosure

C.H. Gibbons serves as a scientific advisor and has stock options in CND Life Sciences. R. Freeman serves as a scientific advisor and has stock options in CND Life Sciences. R. Freeman previously served on the board of directors for CND Life Sciences. The other authors report no relevant disclosures. Go to [Neurology.org/N](https://www.neurology.org/N) for full disclosures.

### Publication History

Received by *Neurology* March 9, 2022. Accepted in final form November 17, 2022. Submitted and externally peer reviewed. The handling editor was Associate Editor Peter Hedera, MD, PhD.

### Appendix Authors

Name	Location	Contribution
<b>Christopher Gibbons, MD, MMSc</b>	Department of Neurology, Beth Israel Deaconess Medical Center, Boston, MA	Drafting/revision of the manuscript for content, including medical writing for content; major role in the acquisition of data; study concept or design; and analysis or interpretation of data
<b>Ningshan Wang, PhD</b>	Department of Neurology, Beth Israel Deaconess Medical Center, Boston, MA	Drafting/revision of the manuscript for content, including medical writing for content; major role in the acquisition of data; and analysis or interpretation of data
<b>Sharika Rajan, MD</b>	Department of Pathology, NIH, Bethesda, MD	Drafting/revision of the manuscript for content, including medical writing for content, and major role in the acquisition of data
<b>Drew Kern, MD</b>	Department of Neurology, University of Colorado, Aurora, CO	Drafting/revision of the manuscript for content, including medical writing for content; major role in the acquisition of data; and analysis or interpretation of data
<b>Jose-Alberto Palma</b>	Department of Neurology, NYU Grossman School of Medicine, NY	Drafting/revision of the manuscript for content, including medical writing for content; major role in the acquisition of data; and analysis or interpretation of data
<b>Horacio Kaufmann, MD</b>	Department of Neurology, NYU Grossman School of Medicine, NY	Drafting/revision of the manuscript for content, including medical writing for content; major role in the acquisition of data; study concept or design; and analysis or interpretation of data
<b>Roy Freeman, MD</b>	Department of Neurology, Beth Israel Deaconess Medical Center, Boston, MA	Drafting/revision of the manuscript for content, including medical writing for content; major role in the acquisition of data; study concept or design; and analysis or interpretation of data

## References

- Wenning GK, Krismer F. Multiple system atrophy. *Handbook Clin Neurol*. 2013;117:229-241. doi: 10.1016/B978-0-444-53491-0.00019-5
- Fanciulli A, Wenning GK. Multiple-system atrophy. *N Engl J Med*. 2015;372(3):249-263. doi: 10.1056/nejmra1311488
- Vekrellis K, Xilouri M, Emmanouilidou E, Rideout HJ, Stefanis L. Pathological roles of alpha-synuclein in neurological disorders. *Lancet Neurol*. 2011;10(11):1015-1025. doi: 10.1016/S1474-4422(11)70213-7
- Wang N, Garcia J, Freeman R, Gibbons CH. Phosphorylated  $\alpha$ -synuclein within cutaneous autonomic nerves of patients with Parkinson's disease: the implications of sample thickness on results. *J Histochem Cytochem*. 2020;68(10):669-678. doi: 10.1369/0022155420960250
- Donadio V, Incensi A, Del Sorbo F, et al. Skin nerve phosphorylated alpha-synuclein deposits in Parkinson disease with orthostatic hypotension. *J Neuropathol Exp Neurol*. 2018;77(10):942-949. doi: 10.1093/jnen/nly074
- Donadio V, Incensi A, Rizzo G, et al. A new potential biomarker for dementia with Lewy bodies: skin nerve alpha-synuclein deposits. *Neurology*. 2017;89(4):318-326. doi: 10.1212/wnl.00000000000004146
- Doppler K, Ebert S, Uceyler N, et al. Cutaneous neuropathy in Parkinson's disease: a window into brain pathology. *Acta Neuropathol*. 2014;128(1):99-109. doi: 10.1007/s00401-014-1284-0
- Donadio V, Incensi A, El-Agnaf O, et al. Skin alpha-synuclein deposits differ in clinical variants of synucleinopathy: an in vivo study. *Sci Rep*. 2018;8(1):14246. doi: 10.1038/s41598-018-32588-8
- Haga R, Sugimoto K, Nishijima H, et al. Clinical utility of skin biopsy in differentiating between Parkinson's disease and multiple system atrophy. *Parkinson's Dis*. 2015;2015:1-7. doi: 10.1155/2015/167038
- Doppler K, Weis J, Karl K, et al. Distinctive distribution of phospho-alpha-synuclein in dermal nerves in multiple system atrophy. *Mov Disord*. 2015;30(12):1688-1692. doi: 10.1002/mds.26293
- Donadio V, Incensi A, Rizzo G, et al. Skin biopsy may help to distinguish multiple system atrophy-parkinsonism from Parkinson's disease with orthostatic hypotension. *Mov Disord*. 2020;35(9):1649-1657. doi: 10.1002/mds.28126
- Gilman S, Wenning GK, Low PA, et al. Second consensus statement on the diagnosis of multiple system atrophy. *Neurology*. 2008;71(9):670-676. doi: 10.1212/01.wnl.0000324625.00404.15
- Hughes AJ, Daniel SE, Lees AJ. Improved accuracy of clinical diagnosis of Lewy body Parkinson's disease. *Neurology*. 2001;57(8):1497-1499. doi: 10.1212/wnl.57.8.1497
- Wenning GK, Tison F, Seppi K, et al. Development and validation of the unified multiple system atrophy rating scale (UMSARS). *Mov Disord*. 2004;19(12):1391-1402. doi: 10.1002/mds.20255
- Goetz CG. [Movement disorder society-unified Parkinson's disease rating scale (MDS-UPDRS): a new scale for the evaluation of Parkinson's disease]. *Revue Neurologique*. 2010;166:1-4. doi: 10.1016/j.neurol.2009.09.001
- Goetz CG, Poewe W, Rascol O, et al. Movement disorder society task force report on the Hoehn and Yahr staging scale: status and recommendations the movement disorder society task force on rating scales for Parkinson's disease. *Mov Disord*. 2004;19(9):1020-1028. doi: 10.1002/mds.20213
- Doty RL, Frye RE, Agrawal U. Internal consistency reliability of the fractionated and whole University of Pennsylvania Smell Identification Test. *Perception Psychophys*. 1989;45(5):381-384. doi: 10.3758/bf03210709
- Gill DJ, Freshman A, Blender JA, Ravina B. The montreal cognitive assessment as a screening tool for cognitive impairment in Parkinson's disease. *Mov Disord*. 2008;23(7):1043-1046. doi: 10.1002/mds.22017
- Kaufmann H, Malamut R, Norcliffe-Kaufmann L, Rosa K, Freeman R. The Orthostatic Hypotension Questionnaire (OHQ): validation of a novel symptom assessment scale. *Clin Auton Res*. 2012;22(2):79-90. doi: 10.1007/s10286-011-0146-2
- Postuma RB, Arnulf I, Hogl B, et al. A single-question screen for rapid eye movement sleep behavior disorder: a multicenter validation study. *Mov Disord*. 2012;27(7):913-916. doi: 10.1002/mds.25037
- Kollensperger M, Geser F, Seppi K, et al. Red flags for multiple system atrophy. *Mov Disord*. 2008;23(8):1093-1099. doi: 10.1002/mds.21992
- Jenkinson C, Fitzpatrick R, Peto V, Greenhall R, Hyman N. The Parkinson's Disease Questionnaire (PDQ-39): development and validation of a Parkinson's disease summary index score. *Age Ageing*. 1997;26(5):353-357. doi: 10.1093/ageing/26.5.353
- Wang N, Gibbons CH. Skin biopsies in the assessment of the autonomic nervous system. *Handbook Clin Neurol*. 2013;117:371-378. doi: 10.1016/B978-0-444-53491-0.00030-4
- Lauria G, Hsieh ST, Johansson O, et al. European Federation of Neurological Societies/Peripheral Nerve Society Guideline on the use of skin biopsy in the diagnosis of small fiber neuropathy. Report of a joint task force of the European Federation of Neurological Societies and the Peripheral Nerve Society. *Eur J Neurol*. 2010;17(7):903-912. doi: 10.1111/j.1468-1331.2010.03023.x
- Gibbons CH, Illigens BMW, Wang N, Freeman R. Quantification of sweat gland innervation: a clinical-pathologic correlation. *Neurology*. 2009;72(17):1479-1486. doi: 10.1212/wnl.0b013e3181a2e8b8
- Nolano M, Provitera V, Caporaso G, Stancanelli A, Vitale DF, Santoro L. Quantification of pilomotor nerves: a new tool to evaluate autonomic involvement in diabetes. *Neurology*. 2010;75(12):1089-1097. doi: 10.1212/wnl.0b013e3181f39cf4
- Koga S, Aoki N, Uitti RJ, et al. When DLB, PD, and PSP masquerade as MSA: an autopsy study of 134 patients. *Neurology*. 2015;85(5):404-412. doi: 10.1212/wnl.0000000000001807
- Miki Y, Foti SC, Asi YT, et al. Improving diagnostic accuracy of multiple system atrophy: a clinicopathological study. *Brain*. 2019;142(9):2813-2827. doi: 10.1093/brain/awz189
- Adler CH, Beach TG, Hentz JG, et al. Low clinical diagnostic accuracy of early vs advanced Parkinson disease: clinicopathologic study. *Neurology*. 2014;83(5):406-412. doi: 10.1212/wnl.0000000000000641
- Adler CH, Beach TG, Zhang N, et al. Clinical diagnostic accuracy of early/advanced Parkinson disease: updated clinicopathologic study. *Neurol Clin Pract*. 2020;11(4):e414-e421. doi: 10.1212/cpj.0000000000001016
- Stankovic I, Quinn N, Vignatelli L, et al. A critique of the second consensus criteria for multiple system atrophy. *Mov Disord*. 2019;34(7):975-984. doi: 10.1002/mds.27701
- Postuma RB, Berg D, Stern M, et al. MDS clinical diagnostic criteria for Parkinson's disease. *Mov Disord*. 2015;30(12):1591-1601. doi: 10.1002/mds.26424
- Donadio V, Incensi A, Rizzo G, et al. Phosphorylated alpha-synuclein in skin Schwann cells: a new biomarker for multiple system atrophy. *Brain*. 2022;awac124. doi: 10.1093/brain/awac124
- Nordcliffe-Kaufmann L, Kaufmann H, Palma JA, et al. Orthostatic heart rate changes in patients with autonomic failure caused by neurodegenerative synucleinopathies. *Ann Neurol*. 2018;83(3):522-531. doi: 10.1002/ana.25170
- Nolano M, Provitera V, Stancanelli A, et al. Small fiber pathology parallels disease progression in Parkinson disease: a longitudinal study. *Acta Neuropathol*. 2018;136(3):501-503. doi: 10.1007/s00401-018-1876-1
- Ayers JL, Lee J, Monteiro O, et al. Different alpha-synuclein prion strains cause dementia with Lewy bodies and multiple system atrophy. *Proc Natl Acad Sci U S A*. 2022;119(6):e2113489119. doi: 10.1073/pnas.2113489119
- Shahnawaz M, Mukherjee A, Pritzkow S, et al. Discriminating alpha-synuclein strains in Parkinson's disease and multiple system atrophy. *Nature*. 2020;578(7794):273-277. doi: 10.1038/s41586-020-1984-7
- Braak H, Tredici KD, Rub U, de Vos RA, Jansen Steur EN, Braak E. Staging of brain pathology related to sporadic Parkinson's disease. *Neurobiol Aging*. 2003;24(2):197-211. doi: 10.1016/S0197-4580(02)00065-9
- Borghammer P, Horsager J, Andersen K, et al. Neuropathological evidence of body-first vs. brain-first Lewy body disease. *Neurobiol Dis*. 2021;161:105557. doi: 10.1016/j.nbd.2021.105557
- Horsager J, Andersen KB, Knudsen K, et al. Brain-first versus body-first Parkinson's disease: a multimodal imaging case-control study. *Brain*. 2020;143(10):3077-3088. doi: 10.1093/brain/awaa238
- Zubelzu M, Morera-Herreras T, Irastorza G, Gomez-Esteban JC, Murueta-Goyena A. Plasma and serum alpha-synuclein as a biomarker in Parkinson's disease: a meta-analysis. *Parkinsonism Relat Disord*. 2022;99:107-115. doi: 10.1016/j.parkrel.2022.06.001
- Singer W, Schmeichel AM, Shahnawaz M, et al. Alpha-synuclein oligomers and neuro-filament light chain in spinal fluid differentiate multiple system atrophy from Lewy body synucleinopathies. *Ann Neurol*. 2020;88(3):503-512. doi: 10.1002/ana.25824
- Donadio V, Wang Z, Incensi A, et al. Vivo diagnosis of synucleinopathies: a comparative study of skin biopsy and RT-QuIC. *Neurology*. 2021;96(20):e2513-e2524. doi: 10.1212/wnl.00000000000011935
- Antelmi E, Pizzi F, Donadio V, et al. Biomarkers for REM sleep behavior disorder in idiopathic and narcoleptic patients. *Ann Clin Transl Neurol*. 2019;6(9):1872-1876. doi: 10.1002/acn3.50833
- McCarter SJ, Sandness DJ, McCarter AR, et al. REM sleep muscle activity in idiopathic REM sleep behavior disorder predicts phenoconversion. *Neurology*. 2019;93(12):e1171-e1179. doi: 10.1212/wnl.00000000000008127
- Doppler K, Jentschke HM, Schulmeyer L, et al. Dermal phospho-alpha-synuclein deposits confirm REM sleep behaviour disorder as prodromal Parkinson's disease. *Acta Neuropathol*. 2017;133(4):535-545. doi: 10.1007/s00401-017-1684-z
- Antelmi E, Donadio V, Incensi A, Plazzi G, Liguori R. Skin nerve phosphorylated alpha-synuclein deposits in idiopathic REM sleep behavior disorder. *Neurology*. 2017;88(22):2128-2131. doi: 10.1212/wnl.0000000000003989

# Neurology®

## Cutaneous $\alpha$ -Synuclein Signatures in Patients With Multiple System Atrophy and Parkinson Disease

Christopher Gibbons, Ningshan Wang, Sharika Rajan, et al.

*Neurology* 2023;100:e1529-e1539 Published Online before print January 19, 2023

DOI 10.1212/WNL.0000000000206772

**This information is current as of January 19, 2023**

<b>Updated Information &amp; Services</b>	including high resolution figures, can be found at: <a href="http://n.neurology.org/content/100/15/e1529.full">http://n.neurology.org/content/100/15/e1529.full</a>
<b>References</b>	This article cites 47 articles, 11 of which you can access for free at: <a href="http://n.neurology.org/content/100/15/e1529.full#ref-list-1">http://n.neurology.org/content/100/15/e1529.full#ref-list-1</a>
<b>Citations</b>	This article has been cited by 1 HighWire-hosted articles: <a href="http://n.neurology.org/content/100/15/e1529.full##otherarticles">http://n.neurology.org/content/100/15/e1529.full##otherarticles</a>
<b>Subspecialty Collections</b>	This article, along with others on similar topics, appears in the following collection(s): <b>Autonomic diseases</b> <a href="http://n.neurology.org/cgi/collection/autonomic_diseases">http://n.neurology.org/cgi/collection/autonomic_diseases</a> <b>Class II</b> <a href="http://n.neurology.org/cgi/collection/class_ii">http://n.neurology.org/cgi/collection/class_ii</a> <b>Multiple system atrophy</b> <a href="http://n.neurology.org/cgi/collection/multiple_system_atrophy">http://n.neurology.org/cgi/collection/multiple_system_atrophy</a> <b>Parkinson's disease/Parkinsonism</b> <a href="http://n.neurology.org/cgi/collection/parkinsons_disease_parkinsonism">http://n.neurology.org/cgi/collection/parkinsons_disease_parkinsonism</a>
<b>Permissions &amp; Licensing</b>	Information about reproducing this article in parts (figures, tables) or in its entirety can be found online at: <a href="http://www.neurology.org/about/about_the_journal#permissions">http://www.neurology.org/about/about_the_journal#permissions</a>
<b>Reprints</b>	Information about ordering reprints can be found online: <a href="http://n.neurology.org/subscribers/advertise">http://n.neurology.org/subscribers/advertise</a>

*Neurology*® is the official journal of the American Academy of Neurology. Published continuously since 1951, it is now a weekly with 48 issues per year. Copyright © 2023 American Academy of Neurology. All rights reserved. Print ISSN: 0028-3878. Online ISSN: 1526-632X.

